ISSN Online: 3007-1941 ISSN Print: 3007-1933
https://msra.online/index.php/Journal/about

Multidisciplinary Surgical Research Annals
https://msra.online/index.php/Journal/about
Volume 3, Issue 2 (2025)

Synthesis and Characterization of Graphene Oxide-Chitosan Based Film Crosslinked with Pectin for Waste Water Treatment

Muhammad Naveed[1*], Faisal Nawaz[2], Yusuf Kyejjusa[3], Muhammad Younas[4],Muhammad Owais[5], Muhammad Yar[6], Saad Ali[7], Samrina Javed[8]

Article Details

Keywords: Graphene oxide, Chitosan, Pectin, Composite, Acetic acid, FTIR, XRD, UV spectroscopy

Muhammad Naveed
Research Scholar, Department of Natural Sciences and Humanities, University of Engineering and Technology Lahore, KSK Campus, Pakistan
Corresponding Author Email: mschemist1998@gmail.com
Faisal Nawaz
Associate Professor, Department of Natural Sciences and Humanities, University of Engineering and Technology Lahore, KSK Campus, Pakistan. Email: faisal.nawaz@uet.edu.pk
Yusuf Kyejjusa
Lecturer, Department Of Chemistry, Islamic University in Uganda (IUIU),
Email: yusuf.kyejjusa@iuiu.ac.ug
Muhammad Younas
Chief Scientist, Oilseeds Research Institute, Faisalabad, Pakistan
Email: dr_y_javed@yahoo.com
Muhammad Owais
Senior Scientist, Wheat Research Institute, Faisalabad, Pakistan
Email: mowais928@gmail.com
Muhammad Yar
Research Scholar, Department Of Chemistry, University of Lahore, Pakistan
Email: muhammadyar1365@gmail.com
Saad Ali
Research Scholar, Department Of Chemistry, University Of Engineering and Technology Lahore, Pakistan. Email: ranjpoot786@gmail.com
Samrina Javed
Research Scholar, Kohat University of Science and Technology, KPK, Pakistan
Email: samrinajaved666@gmail.com

ABSTRACT

In this study, graphene oxide was prepared by using modified hummers method which was cost effective and less time-consuming method. Graphene oxide/Chitosan and Graphene oxide/Chitosan/Pectin composite were prepared by different methods. Pectin dissolved in distilled water and afterward Chitosan solution was made by dissolved in dilute acetic acid solution and graphene oxide in dispersed form combined with it to synthesized two different composite films. The manufactured composite and graphene oxide was characterized with FTIR, XRD and UV spectroscopy. FTIR and XRD results confirmed the successful synthesis of graphene oxide from graphite powder and chitosan/pectin-based composites. The UV results showed that the prepared hydrogels successfully adsorb synozol red from the contaminated water but the composite containing pectin performed better adsorption of synozol red than the composite without pectin and opened a door towards the purification of water.

INTRODUCTION

The vast majority of the dyes that are added to the water system originate from industrial wastewater. These dyes affect aquatic life but also harm the ecosystem as a whole. Because the dyes are readily dissolved in water, they affect food chains and reduce the photocatalytic capabilities of aquatic plants. Dye also makes water unfit for drinking, gardening, and recreational purposes [1]. Hazardous dyes and extremely toxic substances have drawn a lot of attention lately. The majority of researchers seemed to have problems efficiently eliminating organic dyes and hazardous materials from various wastes [2].Dye is a color impart substance which is used for various purposes around the globe. They have two types natural and synthetic. Natural dyes come from plants or minerals while synthetic dyes prepared in laboratory or industry level. Synthetic dyes are classified into anionic, cationic and neutral dyes. Because more people are using cosmetics, textiles, printing, cars, paper, and other materials to add color, the number of companies releasing various dyes has significantly expanded. As a result of these contaminants' growing toxicity and their mixing with potable water supplies, the quality of the source water is declining. Today, over thousands of varieties of dyes are produced commercially [3]. Water pollution has become a pressing global issue, adversely affecting the quality of ground water, surface water. Therefore, water pollution is a serious concern now a days due to increasing utilization of industrial goods [4]. Large amounts of wastewater containing a wide range of color compounds are produced by the textile industry.

Textile industry is the one of the major industries in Pakistan which contributes nearly 20% of total country GDPA. The textile sector waste dyes up to 200,000 tons or above in water streams annually due to unprofessionalism and lack of chemistry knowledge [5, 6]. Degradation or removal of dyes a wide and emerging area of research today [7].

Graphene is atomically thin layer of sp^2 hybridized carbon atoms and could be obtained from graphite. The carbon atoms are arranged in 2-dimensional honey comb like structure [8]. Since last few years' graphene is well known because of its supreme features for numerous applications. Such as transparency [9], thermal conductivity [10], biosensor and good conductor of electricity.

Graphene oxide has hexagonal structure of carbon similar to that of graphene and also contain some of the functional groups based on oxygen such as hydroxyl, carbonyl, alkoxy, and carboxylic acid exhibited in figure (1-A) [11]. Apart from the effortless synthesis, this oxygen based functional groups have many advantages as compared to graphene. One of the advantages include higher solubility [12] and surface functionalization is also possible which opens the door to use in Nano composite materials. Graphene oxide can be converted into reduced graphene oxide by using different techniques, in this way oxygen groups are reduced and pure graphene oxide properties are obtained [13].

In addition to being easy to synthesize, these oxygen-based functional groups are superior to graphene in many ways. Higher solubility [14] and the potential for surface functionalization are two benefits that make nano composite materials a viable option. There are various ways to reduce graphene oxide (GO) to reduced graphene oxide, which reduces oxygen groups and yields pure graphene oxide properties [15].

Researchers in recent years have chosen chitosan, a natural biopolymer, to advance and evolve environmentally friendly biodegradable products [16]. Crustaceans, which include crabs, lobsters, and shrimp, are produced in considerable quantities each year and are eaten as high-protein sea food. Crustacean shells and inedible parts are considered waste; they contain

chitin and protein [17, 18]. The biodegradable polymer, chitosan, is also known as a hydrocolloid. Most hydrocolloids are either neutral or negatively charged at acidic pH values. Nevertheless, the highly reactive amino groups in chitosan give it a positive charge [19]. The desired end product, chitosan, can be produced by deacetylating chitin showed in figure (1-B) [20].

Pectin is a naturally occurring polysaccharide material present in the cell wall of different plants and other peels of citrus materials. Pectin structure is changed according to its source, but mainly comprised repeating units of α-(1-4)-linked D-galacturonic acid units [21]. Due to diversity in their structure, showed numerous novel properties such as their gelation and solubility nature. Furthermore, pectin has ability to remove unwanted substance from wastewater by making different type of hydrogels due to hydrophilic in nature. Pectin based gels made rapidly and provide more thermal stability over other biopolymer like starch, gelatin [22]. Moreover, changing the characteristics of pectin according its degree of methoxylation and acetylation [23]. Pectin provides healthy interaction with water and oil, just because of its amphiphilic [24].

Pectin structure has an extensive multiplicity of physical and chemical effects, which is automatically change its properties and diversely used in different applications. Pectin is a hydrophilic polymer and exhibit swelling properties [25]. The Pectin backbone chain consist of α-(1, 4)-linked D galacturonic acid and also linked by α 1-4 glycosidic bond [26]. Apple Pomace contain Galacturonic acid which comprises of 20 to 44% but orange peel contains have higher content [27]. The structure of pectin could be differed accordingly to its source and methods which is used to extract it. Pectin structure can be methyl-esterified or carboxylated, at 6 position carbon of D-galacturonic acid indicated in Figure (1-C). Carboxyl hydroxyl groups and methylesterified amide groups are hydrophilic and hydrophobic towards metal ions respectively. Therefore, maximum adsorption capacity towards metal ions is much higher when COO^- groups are present more in pectin polysaccharides chain compared to $COOCH_3$ groups [28].

Previously these dyes have been removed from the aqueous solution by different treatments like reverse osmosis, coagulation, adsorption etc. The process of dye removal based on adsorption is considered most efficient because it allows the extended treatment of huge volume of waste water in a cost effective and simple method [29].

In the last few years, hydrogels produced from the hydrophilic polymers were under great interest because of the ability of absorbing water without dissolution. Three dimensional, cross-linked hydrogels can absorb large quantity of water without solving. Owing to their diverse advantage's hydrogels have several applications in agriculture, adsorption and hygienic products [30-32]. More over the hydrogels are capable of changing shape and mobility because of the soft wet material and it is the favorable property as compared to the hard and stiff materials. Infect, hydrogels have wide applications in water treatment because of their superb physical, biological and chemical characteristics. Synthetic as well as natural polymers have been used for the fabrication of vast variety of hydrogels. Hydrogels based on natural resources are more fascinating because of their biodegradability, environment friendly and can be fabricated using low cost process[33].

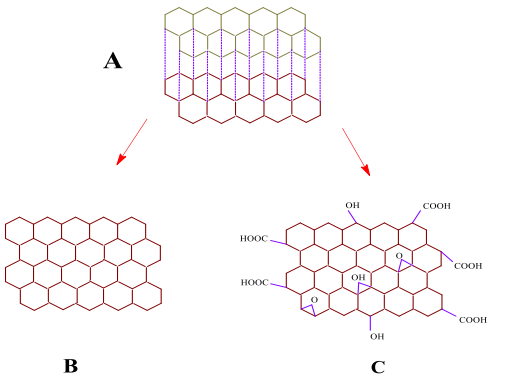

(A)

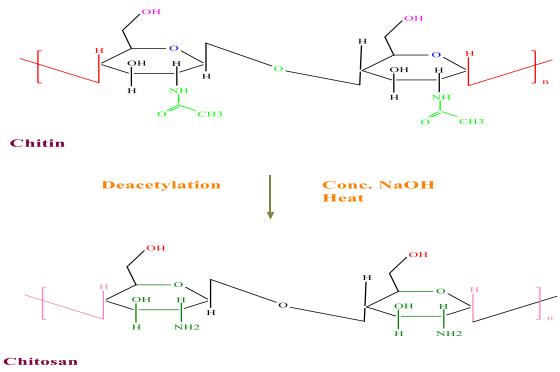

(B)

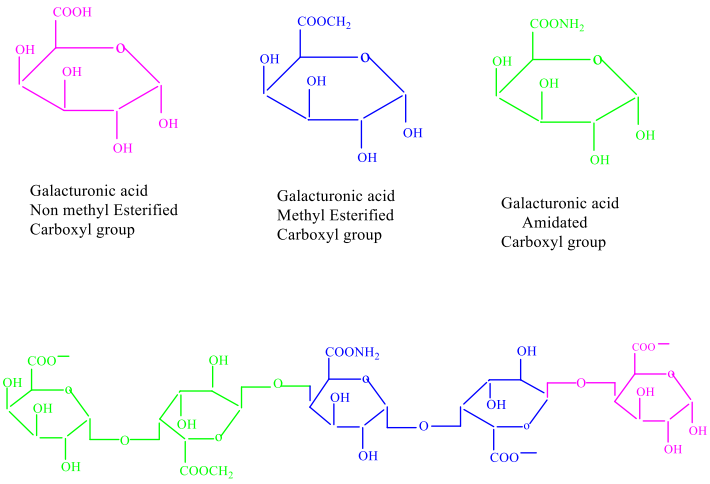

(C)

FIGURE 1: GO (A), CH (B), PEC (C)

EXPERIMENTAL WORK

MATERIALS AND CHEMICALS

Sulphuric acid 98% (Sigma Aldrich), Hydrogen per oxide (Sigma Aldrich), Potassium permanganate (VWR), Sodium nitrate (Sigma Aldrich), Graphite powder (Sigma Aldrich), Hydro- chloric acid 37% (ReAgent), Chitosan (Sigma Aldrich, < 100 kDa), Pectin (Sigma Aldrich, ≥ 74.0%), Synozol red (Interloop textile industry, FSD), Sodium hydroxide (Sigma Aldrich), Acetic acid 0.1 M (ReAgent), Ultrasonicator, Beakers, Thermometer, Conical flask, Graduated cylinder, Eppendorf tubes, Filter paper, Volumetric flask, Pipette, Burette, Iron stand, Glass vials, Zipper bags Funnel, Hot plate with magnetic bar, Centrifuge, Shaker, Analytical balance, Drying oven, Petri dish, Spatula, PH meter.

SYNTHESIS OF GRAPHENE OXIDE

2 grams of graphite powder was mixed with 2 grams of sodium nitrate and 90 ml of sulphuric acid (98%) in 500 ml conical flask, kept under magnetic stirring and ice bath (0-5°C). After the continuous stirring of 4 hrs. 12 grams of potassium permanganate was slowly added to the

suspension to keep the temperature of the reaction mixture below 15˚C. 184 ml of distilled water was slowly added to dilute the reaction mixture and stirred for two hrs. Than ice bath was removed and the mixture was kept under 35˚C and magnetic stirring for two hrs. The reaction mixture is heated to 98˚C for 15 minutes, temperature was decreased to 30˚C after 10 minutes and the brown colored solution was obtained. After 10 min, the reaction mixture is kept at 25˚C for two hrs. Eventually, 40 ml of H_2O_2 is added to the reaction mixture and as a result bright yellow color is obtained. The particles settle down as the reaction mixture is kept without stirring for 2 days. Finally, the sample was washed with 10% HCl solution and deionized water several times until the pH became neutral [34].

FABRICATION OF GRAPHENE OXIDE/CHITOSAN (GO/CH) COMPOSITE

Graphene oxide contains oxygenated functional groups on its surface that why dispersed in water easily. 0.05 g of GO was dispersed in 30 ml of distilled water and ultra-sonicated for 20 min. 2g chitosan was dissolve in 150 ml of 1% acetic acid in a separate flask and continued stirring for 12 to 18 hrs. After that the temperature of chitosan solution was raised to 60˚C and the homogeneous suspension of graphene oxide showing dark brown color, was mixed with chitosan aqueous solution under vigorous stirring. The stirring continued for 6 hrs. Until the viscous liquid formed. The resulting liquid is than poured into Petri dish and dried at 60˚C in an air oven [35].

FABRICATION OF GRAPHENE OXIDE/CHITOSAN/PECTIN (GO/CH/PEC) COMPOSITE

A conical flask containing 100 mL of 1% acetic acid and 1 g of chitosan was continuously stirred. 100 mL of distilled water were used to dissolve 0.25 g of pectin powder, and the liquid was stirred until it was homogenous. Afterward 0.1g graphene oxide was added into chitosan solution. After GO added, 10 mL of chitosan solution was added dropwise into 100 mL of pectin solution and stirring was continued 1 hour. The mixture was stirred, then transferred to a petri dish and dried for 24 hours at 60°C in an oven. The sample was removed from the petri dish after 24 hours drying period, yielding a thin layer of GO/CH/PEC [36].

CHARACTERIZATION

FT-IR ANALYSIS

The FTIR spectrum of the films was measured using Fourier Transform Infrared spectrophotometer (Agilent Cary 630) to investigate the bonding interaction in graphene oxide. The samples were analyzed within the range of 650–4000 cm^{-1} with resolution of 16 cm^{-1} and scanning times 96 at room temperature.

XRD ANALYSIS

The crystal phases of the developed films was examined by X-ray diffractometer (Bruker D8 DISCOVER) within the 2θ range of 5–60° with steps of 5°/min. The analysis was conducted to know about the structural and crystalline properties of the composite film [37].

SWELLING INDEX

The water absorbing capacity of hydrogels was determined. The small pieces of hydrogels were weighed and added in 50 ml of distilled water in a petri dish. After every 10 minutes the water in petri dish was removed and the petri dish containing the hydrogel was dried with tissue paper.

The percentage swelling of both hydrogels after equilibrium, was determined using the formula

$$\text{Swelling } (\%) = \frac{W1 - W0}{W0}$$

Where W_0 was the initial mass and W_1 was the final mass of composite film. [38].

MOISTURE CONTENT

To measure the moisture retention capacity, the prepared composite films were cut in equal pieces and weighed. The film samples were placed in on oven at 105°C for 6 hrs. The hydrogels were again weighed after 6 hrs.

$$\text{Moisture retention capacity (\%)} = \frac{W1 - W6hrs}{W1} \times 100$$

Where, W_{6hrs} is weight in g after 6 hrs. and W_1 is representing the initial weight.[39]

WATER SOLUBILITY

To measure water solubility, identical pieces of composite film were cut, then placed in oven at 105°C to obtain their weight constant. After the constant weight was obtained the dried film samples were placed in DI water for 24h. The film samples were now again placed in oven until the constant weight was obtained.

$$WS\ (\%) = \frac{W0 - W1}{W0} \times 100$$

Where, W_0 is theinitial weight and W_1 is the final weight of the film samples [40].

APPLICATION OF COMPOSITE FILMS FOR SYNOZOL RED DYE DEGRADATION BY UV-VIS SPECTROPHOTOMETER

The experiment was carried out to check the adsorption mechanism of prepared composite films by using the shaker with the speed of 180 rpm. First 50 ppm stock solution of synozol red was prepared. The stock solution of synozol red was diluted to 10 and 15 ppm to carry out the absorption test. 50 ml of synozol red solution was taken into a glass flask and weight of composite film samples 0.030 g were added into the flask containing the synozol red solution and shook at room temperature. After every 20-minute interval, a sample was taken and the concentration of synozol red in each sample was measured by UV spectrophotometer.

RESULTS AND DISCUSSION

FT-IR ANALYSIS

There is a noticeable peak at 3362 cm-1 in the FTIR spectrum of chitosan due to the –OH stretching vibrations. The peaks at 2990 and 2862 cm-1, respectively, reflected C-H symmetric and asymmetric stretching. The peaks that formed at 1650 and 1423 cm-1 were attributed to the C=O stretching of amide I and the C-N stretching of amide III, respectively, suggesting that chitosan is not completely deacetylated. Accordingly, the peaks at 1587 and 1148 cm-1 are caused by the N-H bending of the primary amine and the asymmetric stretching of the C-O-C bond [41].

The C-OH bond, represented by the peak at 1056 cm-1 in the GO spectrum. The signal at 1623 cm-1 verified that the C=C bond remains intact during oxidation. The peak at 1386 cm^{-1} represents the C-O bond verifies the existence of an oxide functional group. The broad peak at 3410 cm^{-1} showed the O-H bond and absorbed water in GO [42].

The -OH stretching vibration caused by the intra- and intermolecular hydrogen bonding of the galacturonic acid is seen in the pectin FTIR spectrum as a peak at 3392 cm-1. Peaks at 1636 and 1438 cm-1 are caused by the carboxylic group's symmetrical and asymmetrical vibrations, respectively, whilst peaks at 2944 and cm-1 are caused by the C-H bond's stretching vibration. At 1740 cm-1, a peak representing the carboxylic group's methyl ester's C=O stretching vibration is visible. The remaining bands at 1148 and 1015 cm-1 are caused by the stretching vibrations of the C-OH groups and the C-O-C glycosidic bonds, respectively [43].

In the FTIR spectrum of GO/CH blend the peak at 3206.16 cm^1 represented the

stretching of-NH from chitosan and OH of the graphene oxide. The band at 1152.29 cm^{-1} and 1019.14 cm^{-1} represented the secondary and primary alcoholic group respectively. The peak at 894.52 cm^{-1} represented the pyranose ring and chitosan saccharide structure are at 1152.29 cm^{-1}. The peak of C-O of C-O-C was represented in the area of 1064.09 cm^{-1}. Peak at 1548 cm^{-1} showed NH bending of NH2 and peak at 1405 cm^{-1} represented C-OH group [44].

The peaks at 1072 and 1025 cm-1, respectively, of GO/CH/PEC represent the C-O and C-C stretching vibrations of pectin and chitosan. A band at 1754 cm-1 that has shifted toward 1740 cm-1 indicates the ester carbonyl stretching vibration of pectin. Peaks at 1634 and 1554 cm-1 correspond to the amide -CO stretching and -NH bending vibrations, which confirm the electrostatic interactions between the amino group of chitosan and the carboxyl group of

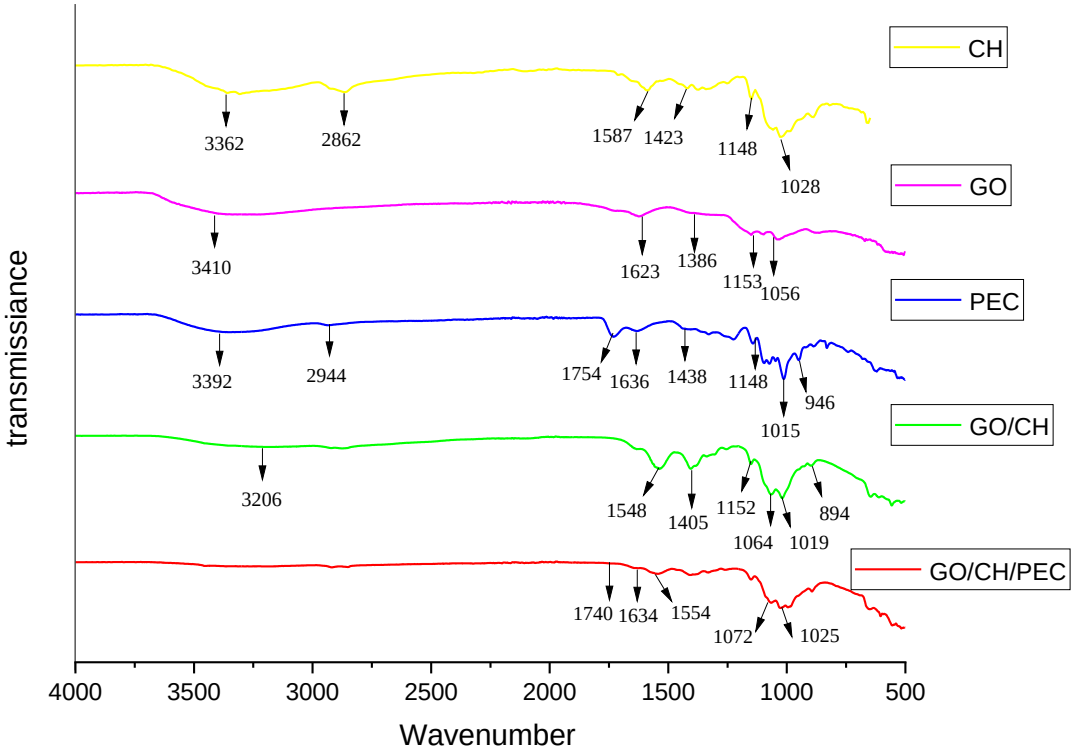

pectin. The rise in GO concentration, however, combines with the peaks observed at 1634 and 1554 cm-1. Strong hydrogen bonds between GO and pectin as well as ionic interactions between the -NH3 group of chitosan and the -COO-groups of both pectin and GO may be the cause of this finding [45].

Figure 3.1Graphical showed FTIR Spectrum of CH, GO, PEC, GO/CH, GO/CH/PEC

XRD ANALYSIS

XRD spectra of chitosan was showed peak at $2\theta = 19.7°$. Its semi-crystalline structure was indicated by the peaks in the chitosan XRD pattern [46]. The XRD pattern of pectin is displayed, with its distinctive crystalline peak located at $2\theta = 13.0°$, 18.7°, 20.0°, 24.6°, and 38.1° [47]. XRD results peaks of GO was showed at $2\theta = 8.0°$ and 26.3°. The graph exhibited a sharp peak at $2\theta = 8.0°$ confirming that graphite powder was oxidized well by mean of concentrated acids and KMnO4 and obtained GO [48].

The crystalline nature of GO film peak slightly changes and was exhibited a peak at $2\theta = 8.7°$ after the incorporation with CH because of the diffraction overlap. Other peaks of GO/CH

exhibited at 2θ = 12° and 18.6°. These results highly appreciated by previous literatures [49]. CH and GO composite film consist of a combination of crystalline and amorphous nature. It represents that the extent of physical interaction is greater and the extent of chemical interaction between chitosan and graphene oxide is lower. In the case of GO/CH/PEC composite, no characteristic peaks for GO were observed. The lack of peaks that correspond to GO is well distributed throughout the polymer matrix. Both pectin and chitosan's distinctive peaks disappeared, while new ones emerged at 2θ = 12.1°, 15.2° and 20.8°. The crystalline property of the individual polymers may be diminished as a result of the electrostatic contact between the polymers. In some cases, sometimes shoulder peaks also appeared in XRD peaks due to strong interaction between different materials and its crystallinity features.

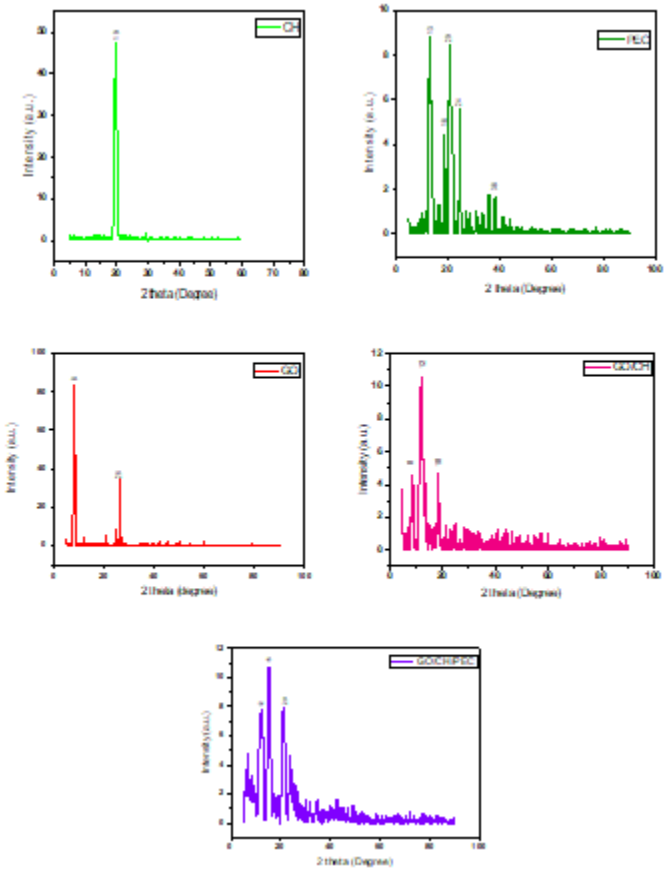

FIGURE 3.2 EXHIBITED XRD SPECTRUMS OF CH, PEC, GO, GO/CH AND GO/CH/PEC

SWELLING INDEX

The GO/CH/PEC film show greater swelling as compared to GO/CH film because increase hydrophilicity of film by addition of pectin which carried hydrophilic galacturonic acid units and methoxyl groups. The presence of functional groups (-OH, -COOH, -NH_2) in all three materials enables more hydrogen bonding and ionic interactions, which strengthen composite network and increase its swelling capacity.

Using the formula SI = $\frac{S0-S1}{S0}$ x 100 the GO/CH/PEC composite was showed the maximum swelling of 25%, whereas the GO/CH composite showed the maximum swelling of 20%.

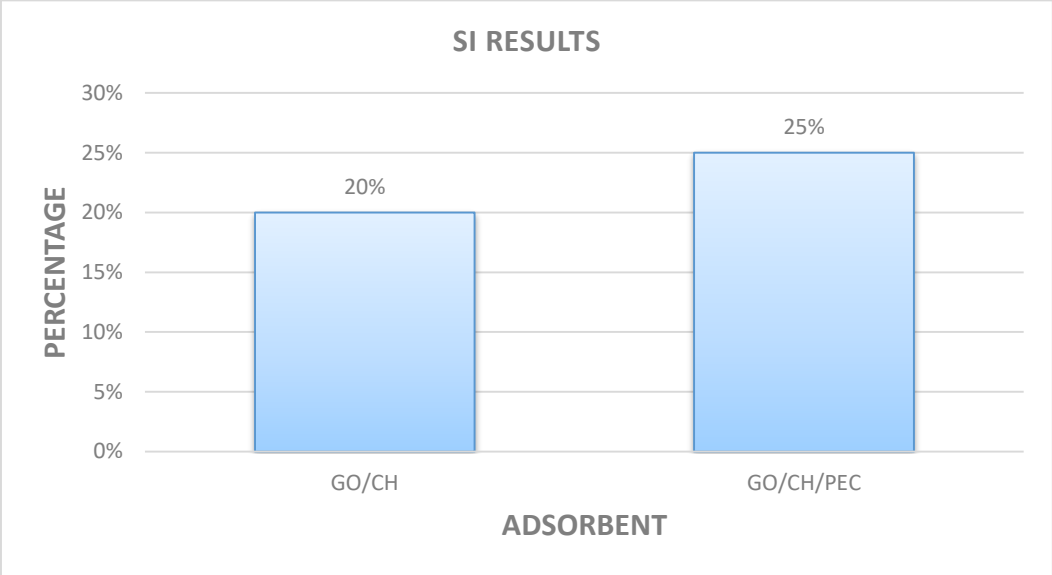

FIGURE 3.3 GRAPHICAL EXHIBITED SWELLING INDEX RESULTS

WATER SOLUBILITY

When using composite films for dye degradation, it is crucial to take into account their water solubility parameter. The water solubility of the both synthesized films were recorded by using this formula WS = $\frac{S0-S1}{S0}$ x 100.GO/CH/PEC film exhibits a water solubility of 15.5%, which is somewhat greater than the 8.33% of GO/CH composite film. This is because both pectin and chitosan are hydrophilic; however, adding pectin to a GO/CH composite film may developed more hydrophilicity character which would increase the film's water solubility.

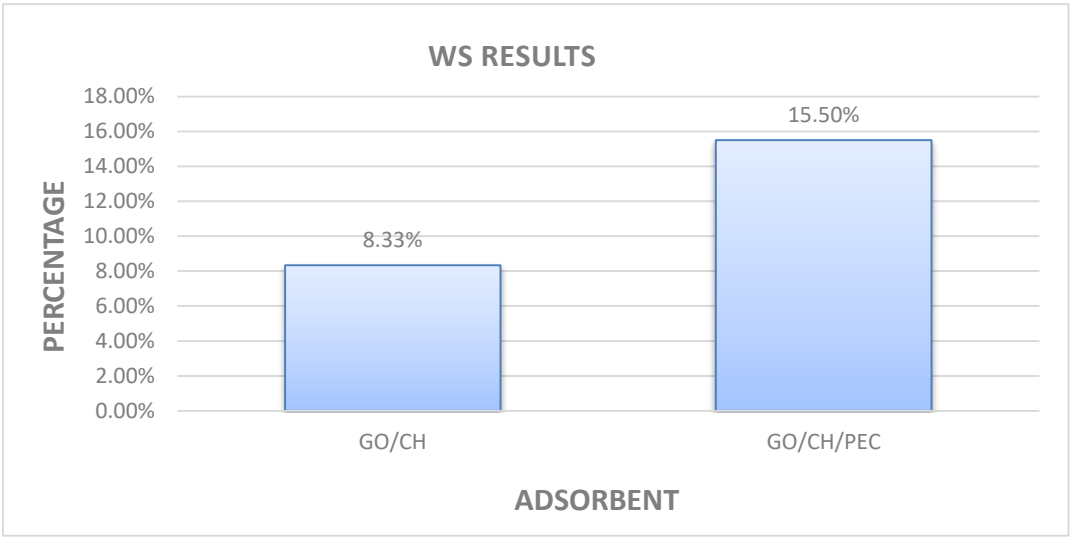

FIGURE 3.4 GRAPHICAL REPRESENTATION OF WATER SOLUBILITY

MOISTURE CONTENT

Compared to GO/CH film, GO/CH/PEC film exhibits higher MC, which could be because PEC increases the composite hydrophilicity. In comparison to chitosan, pectin has more (-OH) groups. These hydroxyl groups have the potential to create hydrogen bonds with water molecules, which would raise the composite's MC. The moisture content of the both synthesized films were recorded by using the moisture content formula MC = $\frac{S0-S1}{S0}$ x 100.

GO/CH film MC value was showed 3.4% whereas GO/CH/PEC showed 4.3%.

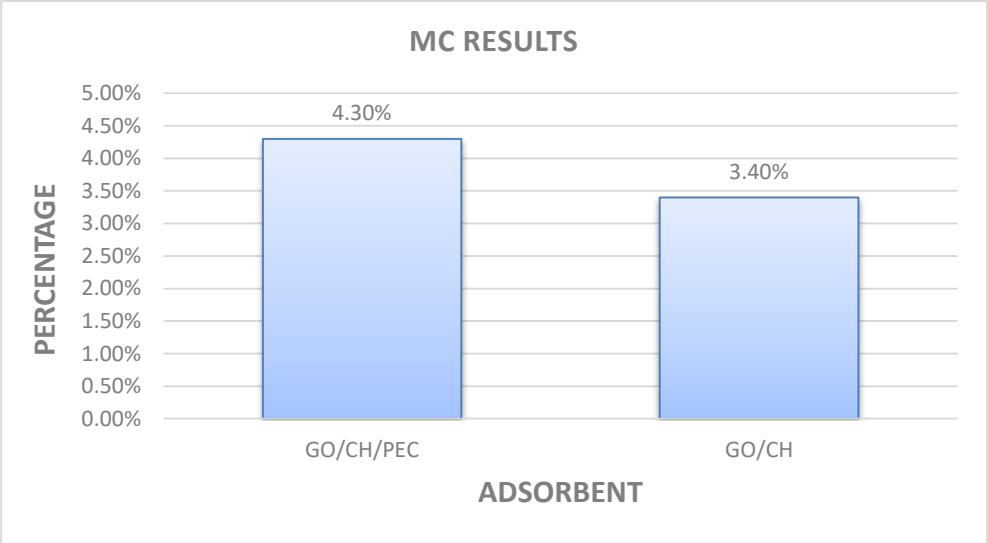

FIGURE 3.5 GRAPHICAL REPRESENTATION OF MOISTURE CONTENT

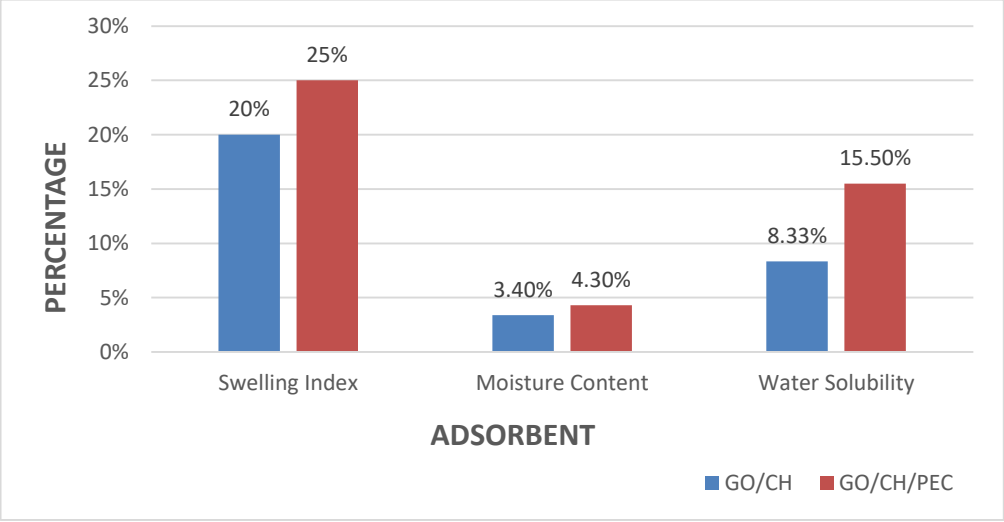

FIGURE 3.6 PERCENTAGE REPRESENTATION OF DIFFERENT TESTS

Table 1

%	GO/CH	GO/CH/PEC
Moisture content	3.40	4.30
Swelling index	20	25
Water solubility	8.33	15.50

BATCH ADSORPTION EXPERIMENT

In order to determine how various parameters, including pH and starting concentration, affected the thin composite films' ability to adsorb synozol red dye, an adsorption test was conducted.

EFFECT OF PH ON ADSORPTION

Synozol red dye adsorption on prepared thin films was investigated at pH 3, 7 and 11 and the samples were investigated after every 20 minutes' interval or called batch method. Moreover, we were taking 50 ml of synozol red dye solution for two films separately in two different beakers and then 0.030 weight of each composite film was added in beakers accordingly. At pH 7, there was 85.91% degradation by GO/CH and 92.95% degradation by GO/CH/PEC However, at pH 3 there was 60.56 % and 98.59% degradation by GO/CH and GO/CH/PEC respectively. At pH 11, 15% of the dye was removed by GO/CH and 17.60 % removed by GO/CH/PEC.

The GO/CH/PEC composite showed better dye degradation than the GO/CH compositeatdifferentpH.AtpH3pectinbasedcompositefilmwasshowedmorethan 90%degradationofsynozolreddyeduetotheenhancedsurfacechargedensity,which improvesstabilityanddispersion,andthestronghydrogenbondsthatformbetweenthe dye molecules and the pectin's hydroxyl groups are responsible for this enhancement. Chitosan structure diminished under strong acidic medium, this may lead to decrease the degradation rate as compared to GO/CH/PEC composite in acidic medium. At pH 11, the reduced adsorption of Synozol Red dye by both films could be attributed to the deprotonation offunctionalgroups,whichleadstoincreasedelectrostaticrepulsion,diminished hydrogen bonding, and enhanced dye solubility. These factors collectively contribute to the decreased adsorption rate.

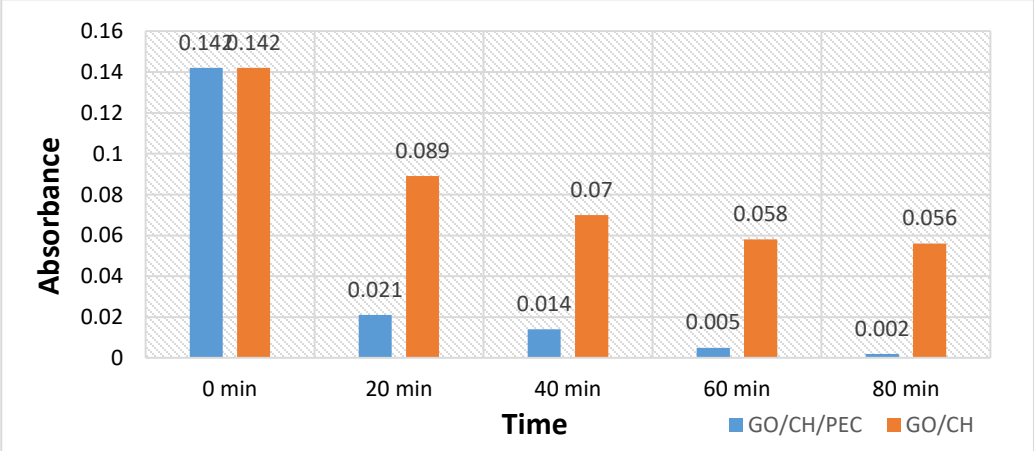

FIGURE 3.7 GRAPHICAL REPRESENTED OF DYE DEGRADATION AT 3 PH

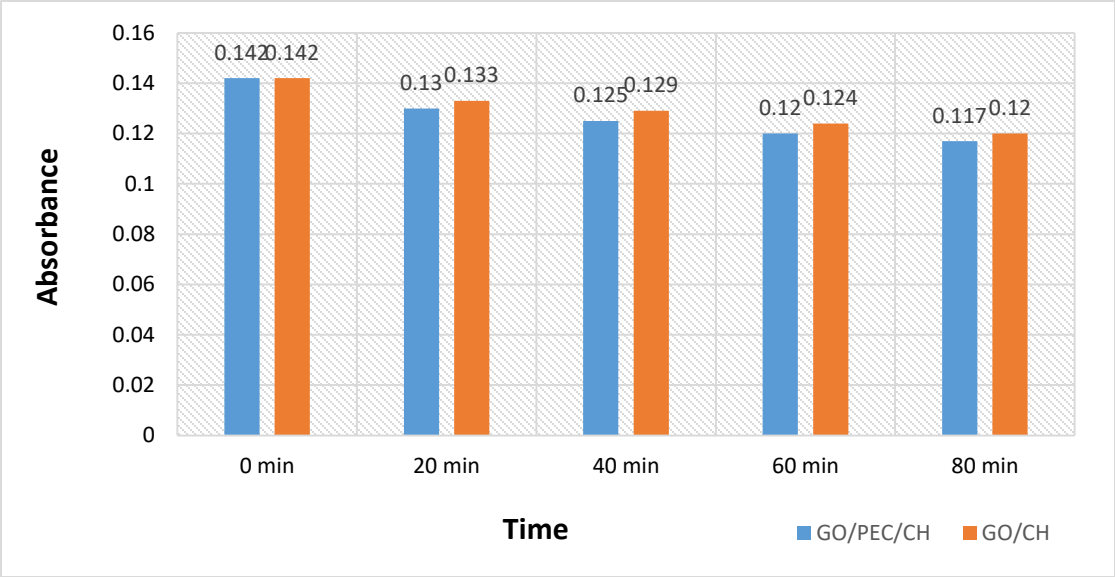

FIGURE 3.8 GRAPHICAL REPRESENTED OF DYE ADSORPTION AT PH 11

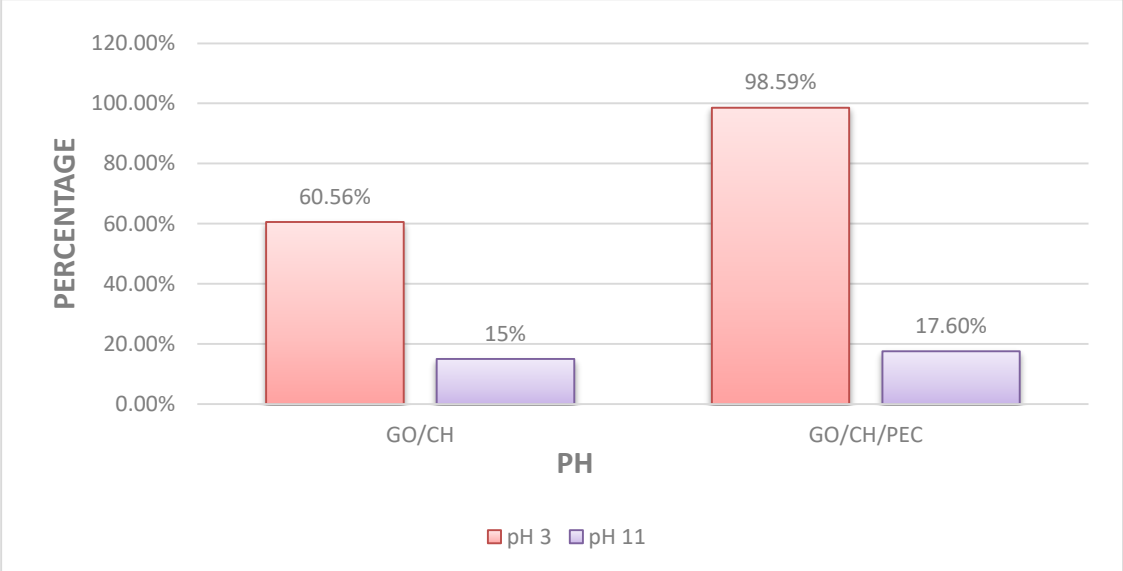

FIGURE 3.9 GRAPHICAL SHOWED % DEGRADATION AT DIFFERENT PH

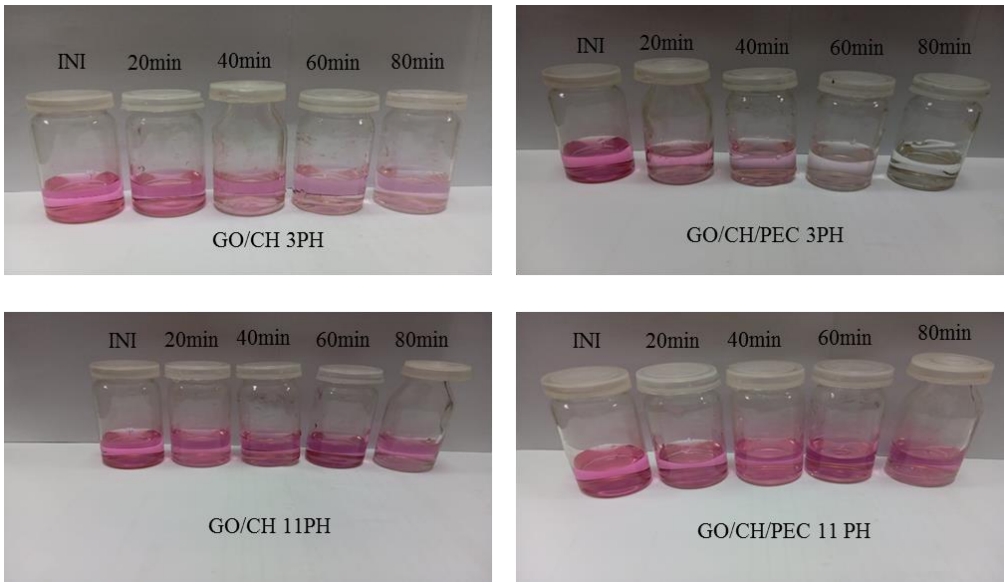

FIGURE 3.10 IMAGES SHOWED THAT CHANGING THE DYE COLOR AFTER EVERY 20 MINUTES INTERVAL

TABLE 02

Adsorbent Sample	pH 3	pH 11
GO/CH	60.56%	15%
GO/CH/PEC	98.59%	17.60%

EFFECT OF INITIAL CONCENTRATION OF SYNOZOL RED

At constant pH (7) and adsorbent mass (0.030) for each film, the effect of synozol red concentration was studied at 10 ppm and 15 ppm concentration. We have already mentioned,atneutralpHbothfilmswereexhibitedgoodadsorbentfordyedegradation. GO/CH was showed 78.87% dye degradation at 10 ppm while GO/CH/PEC was exhibited 85.91% dye degradation at the same time and concentration as well. Furthermore, GO/CH was showed 83.56% dye degradation at 15 ppm while GO/CH/PEC was exhibited 87.32% dye degradation.

According to results, at pH 7 both composite films were exhibited good adsorption rate due to electrostatic attraction between the negatively charged dye moleculesandtheGO/CHandGO/CH/PECcomposites functional groups.Furthermore,pectinhasmore negatively charged functional groups, but may be attributed to pectin based hydrophobic surface which could interact with the hydrophobic part of the dye moleculescouldbemoreeffectivelydegradationofthedyemolecules.Additionally,π- π interactions between GO and dye molecules could be good adsorption and degradation of the dye Molecules.

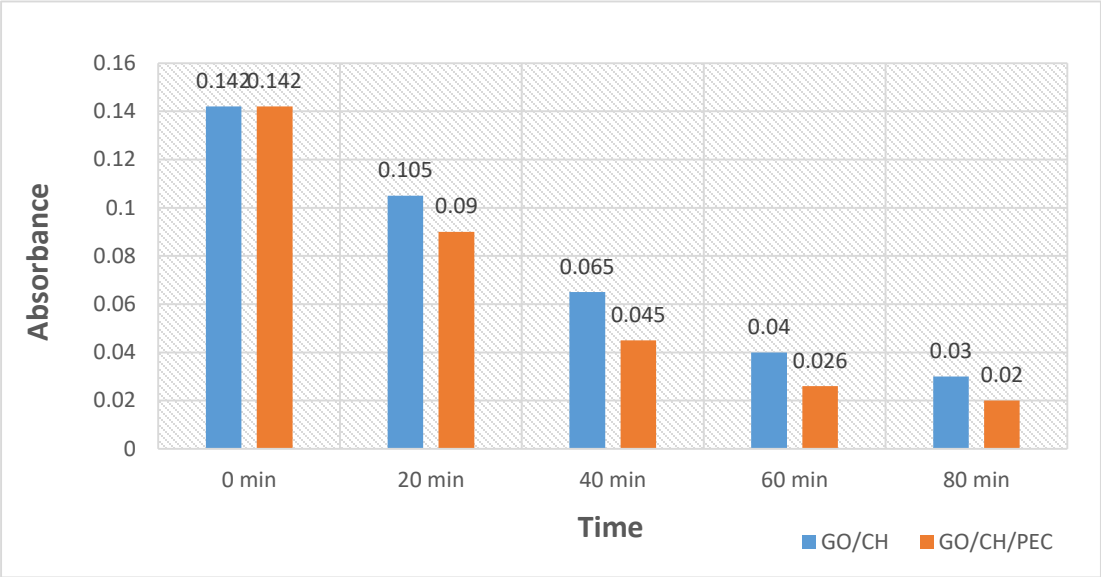

FIGURE 3.11 GRAPHICAL REPRESENTED OF ADSORPTION AT 10 PPM

Hence, when the sample was exposed to UV light without the composite film, there was no discernible difference between the initial and final dye concentrations. This could be because there was no photocatalytic activity to start the dye molecules' breakdown.Intheabsenceofcompositefilm,noreactiveoxygenspeciesareproduced, which is why dye molecules do not break down under UV without composite films.

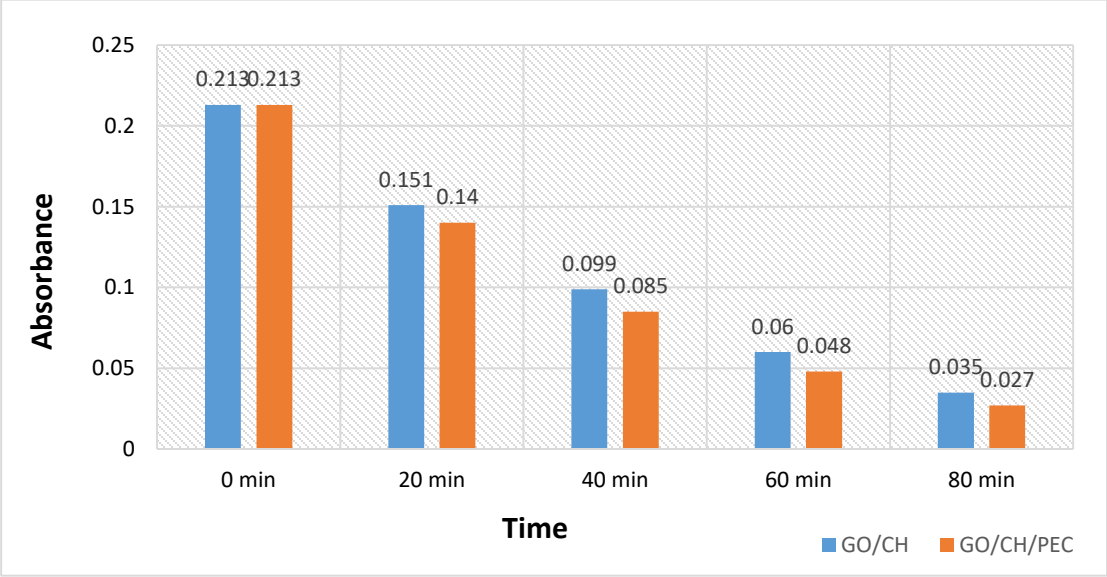

FIGURE 3.12 GRAPHICAL REPRESENTED OF ADSORPTION AT 15 PPM

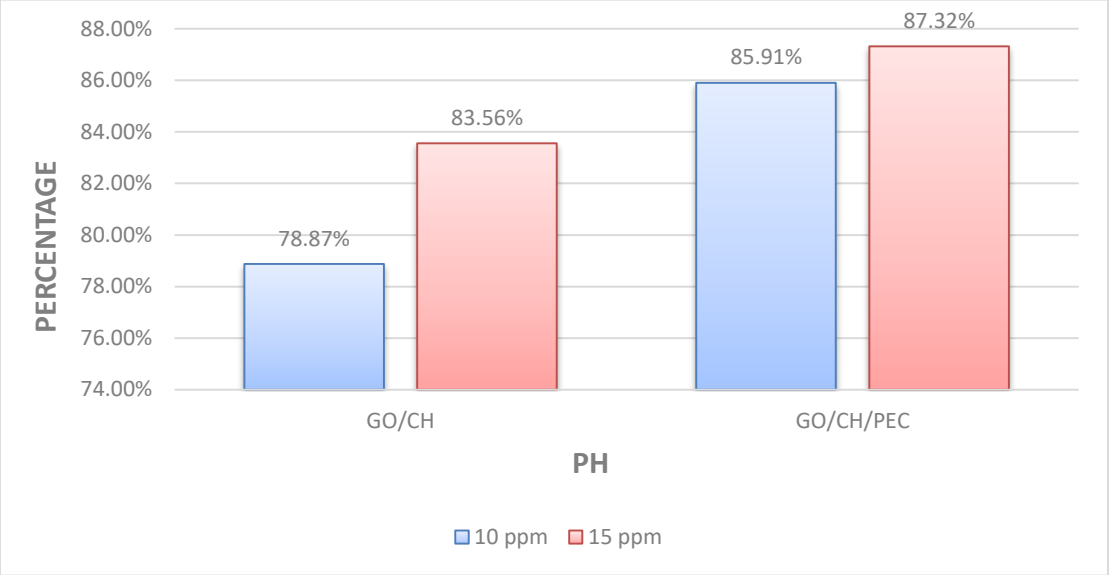

FIGURE 3.13 GRAPHICAL EXHIBITED % DEGRADATION AT DIFFERENT CONCENTRATION

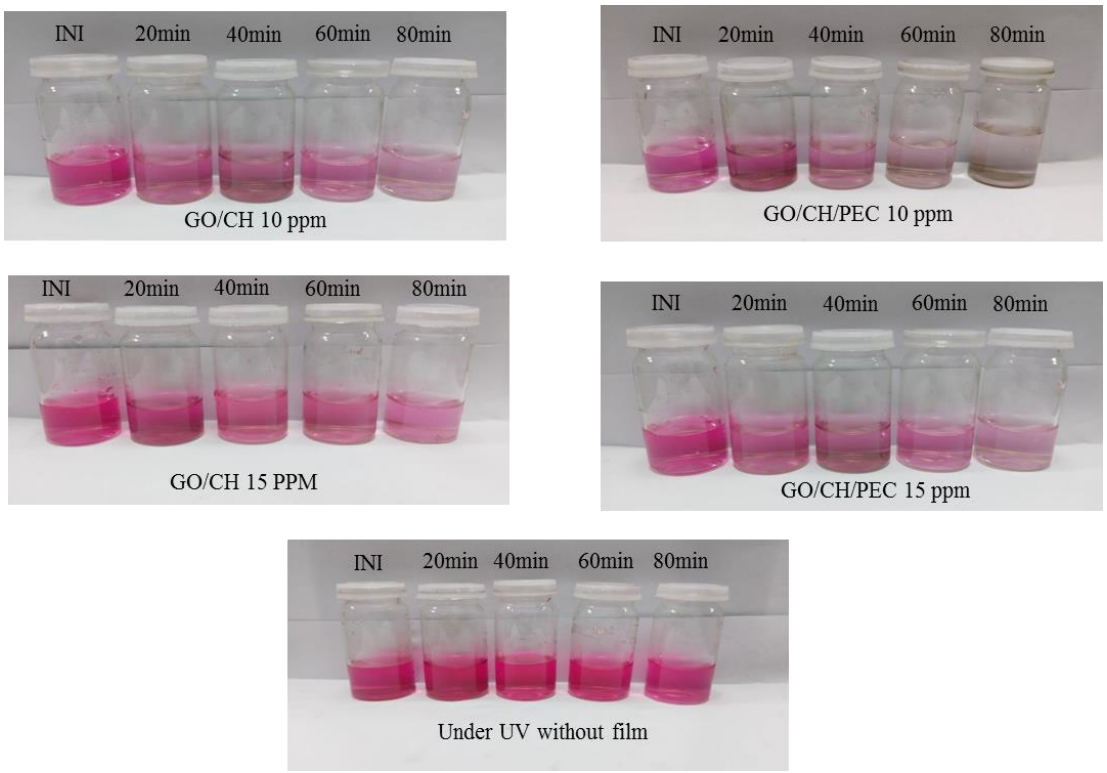

FIGURE 3.14 IMAGES SHOW THAT CHANGING THE DYE COLOR AFTER EVERY 20 MINUTES INTERVAL AT DIFFERENT DYE CONCENTRATION

TABLE 03

Adsorbent Sample	10 ppm	15 ppm
GO/CH	78.87%	83.56%
GO/CH/PEC	85.91%	87.32%

CONCLUSION

This work used a modified Hummers method to successfully manufacture graphene oxide. Successful fabrication of composite films based on graphene oxide was also achieved. FTIR spectrum showed the successful preparation of graphene oxide from graphite powder. The FTIR spectrum of composite films confirmed the uniform blending of graphene oxide, chitosan and pectin. The results of water solubility test, moisture content and swelling index showed that the composite films with pectin produce maximum results other than composite film without pectin. The degradation of synozol red from contaminated dye water more than 80% by using thin composite films was confirmed by UV spectrophotometer. The UV results showed that GO/CH/PEC performed the degradation process more efficiently when we were used 10 ppm and 15 ppm concentration of dye solution. Furthermore, pectin has more negatively charged functional groups, but may be attributed to pectin based hydrophobic surface which could interact with the hydrophobic part of the dye molecules could be more effectively degradation of the dye molecules. Additionally, π-π interactions between GO and dye molecules could be good adsorption and degradation of the dye Molecules. On the other hand, in highly acidic medium which also helped the dye molecules degrade up to 98% or could be more by the GO/CH/PEC composite. This is because of due to the enhanced surface charge density, which improves stability and dispersion, and the strong hydrogen bonds that form between the dye molecules and the pectin's hydroxyl groups are responsible for this enhancement. Chitosan structure diminished under strong acidic medium, this may lead to decrease the degradation rate as compared to GO/CH/PEC composite. GO/CH as well as GO/CH/PEC both were not produced good results in highly basic medium due to deprotonation of functional groups, which leads to increased electrostatic repulsion, diminished hydrogen bonding. By effectively purifying dye-containing contaminated water, this innovation made it possible to reuse a significant amount of industrial waste water.

The findings of this study demonstrate the efficacy of GO/CH crosslinked with Pectin in degradation of dyes from wastewater. The varying composites exhibited distinct degradation performances, highlighting the importance of optimizing material composition for enchased dye removal efficiency. Notably, the synergistic effects of graphene oxide, chitosan and pectin led to improved degradation rates, underscoring the potential of these hybrid materials for sustainable wastewater treatment solution.

This research contributes to the development of innovative, efficient, and composites could be developed from peels and other waste materials for mitigating the dye-based pollution, ultimately promoting a cleaner and more sustainable water future.

REFERENCE

1. Stankovich, S., Dikin, D. A., Dommett, G. H., Kohlhaas, K. M., Zimney, E. J., Stach, E. A., ... & Ruoff, R. S. (2006). Graphene-based composite materials. *nature*, *442*(7100), 282-286.
2. Qi, Y., Deng, B., Guo, X., Chen, S., Gao, J., Li, T., ... & Liu, Z. (2018). Switching vertical to horizontal graphene growth using faraday cage- assisted PECVD approach for high- performance transparent heating device. *Advanced materials*, *30*(8), 1704839.
3. Date, M., & Jaspal, D. (2024). Dyes and heavy metals: removal, recovery and wastewater

reuse—a review. *Sustainable Water Resources Management*, *10*(2), 90.)

4. Qi, Y., Deng, B., Guo, X., Chen, S., Gao, J., Li, T., ... & Liu, Z. (2018). Switching vertical to horizontal graphene growth using faraday cage- assisted PECVD approach for high- performance transparent heating device. Advanced materials, 30(8), 1704839.
5. George, G., Ealias, A. M., & Saravanakumar, M. P. (2024). Advancements in textile dye removal: a critical review of layered double hydroxides and clay minerals as efficient adsorbents. Environmental Science and Pollution Research, 31(9), 12748-12779.)
6. Islam, T., Repon, M. R., Islam, T., Sarwar, Z., & Rahman, M. M. (2023). Impact of textile dyes on health and ecosystem: A review of structure, causes, and potential solutions. Environmental Science and Pollution Research, 30(4), 9207-9242.
7. Selvaraj, V., Karthika, T. S., Mansiya, C., & Alagar, M. (2021). An over review on recently developed techniques, mechanisms and intermediate involved in the advanced azo dye degradation for industrial applications. *Journal of molecular structure*, *1224*, 129195.
8. Stankovich, S., Dikin, D. A., Dommett, G. H., Kohlhaas, K. M., Zimney, E. J., Stach, E. A., ... & Ruoff, R. S. (2006). Graphene-based composite materials. nature, 442(7100), 282-286.
9. Qi, Y., Deng, B., Guo, X., Chen, S., Gao, J., Li, T., ... & Liu, Z. (2018). Switching vertical to horizontal graphene growth using faraday cage- assisted PECVD approach for high- performance transparent heating device. Advanced materials, 30(8), 1704839.
10. Ma, T., Gao, H. L., Cong, H. P., Yao, H. B., Wu, L., Yu, Z. Y., ... & Yu, S. H. (2018). A bioinspired interface design for improving the strength and electrical conductivity of graphene- based fibers. Advanced materials, 30(15), 1706435.
11. Pendolino, F., & Armata, N. (2017). Graphene Oxide in Environmental Remediation Process. SpringerBriefs in Applied Sciences and Technology. doi:10.1007/978-3-319-60429-9
12. Kuilla, T., Bhadra, S., & Dahu, Y. (2010). Kim NH, Bose S., Lee JH. Prog. Polym. Sci, *35*(1350), 4.
13. Pei, S., & Cheng, H. M. (2012). The reduction of graphene oxide. Carbon, 50(9), 3210-3228.
14. Kuilla, T., Bhadra, S., Yao, D., Kim, N. H., Bose, S., & Lee, J. H. (2010). Recent advances in graphene based polymer composites. *Progress in polymer science*, *35*(11), 1350-1375.
15. Pei, S., & Cheng, H. M. (2012). The reduction of graphene oxide. *Carbon*, *50*(9), 3210-3228.
16. Tang, Y. F., Du, Y. M., Hu, X. W., Shi, X. W., & Kennedy, J. F. (2007). Rheological characterisation of a novel thermosensitive chitosan/poly (vinyl alcohol) blend hydrogel. *Carbohydrate Polymers*, *67*(4), 491-499.
17. Tsigos, I., Martinou, A., Kafetzopoulos, D., & Bouriotis, V. (2000). Chitin deacetylases: new, versatile tools in biotechnology. *Trends in biotechnology*, *18*(7), 305-312.
18. Crini, G. (2006). Non-conventional low-cost adsorbents for dye removal: a review. *Bioresource technology*, *97*(9), 1061-1085.
19. Kumirska, J., Czerwicka, M., Kaczyń ski, Z., Bychowska, A., Brzozowski, K., Thöming, J., & Stepnowski, P. (2010). Application of spectroscopic methods for structural analysis of chitin and chitosan. *Marine drugs*, *8*(5), 1567-1636.
20. Li, X., Zhou, H., Wu, W., Wei, S., Xu, Y., & Kuang, Y. (2015). Studies of heavy metal ion adsorption on Chitosan/Sulfydryl-functionalized graphene oxide

composites. *Journal of colloid and interface science*, *448*, 389-397.

21. Olawuyi, I. F., Kim, S. R., Hahn, D., & Lee, W. Y. (2020). Influences of combined enzyme-ultrasonic extraction on the physicochemical characteristics and properties of okra polysaccharides. Food Hydrocolloids, 100, 105396.
22. Said, N. S., Olawuyi, I. F., & Lee, W. Y. (2023). Pectin hydrogels: Gel-forming behaviors, mechanisms, and food applications. Gels, 9(9), 732.
23. Belkheiri, A., Forouhar, A., Ursu, A. V., Dubessay, P., Pierre, G., Delattre, C., ... & Michaud, P. (2021). Extraction, characterization, and applications of pectins from plant by-products. Applied Sciences, 11(14), 6596.
24. Humerez-Flores, J. N., Verkempinck, S. H., De Bie, M., Kyomugasho, C., Van Loey, A. M., Moldenaers, P., & Hendrickx, M. E. (2022). Understanding the impact of diverse structural properties of homogalacturonan rich citrus pectin-derived compounds on their emulsifying and emulsion stabilizing potential. Food Hydrocolloids, 125, 107343.
25. Sultana, N. (2023). Biological Properties and Biomedical Applications of Pectin and Pectin-Based Composites: A Review. Molecules, 28(24), 7974.
26. Ropartz, D., & Ralet, M. C. (2020). Pectin structure. Pectin: Technological and physiological properties, 17-36.
27. Cui, J., Zhao, C., Feng, L., Han, Y., Du, H., Xiao, H., & Zheng, J. (2021). Pectins from fruits: Relationships between extraction methods, structural characteristics, and functional properties. Trends in Food Science & Technology, 110, 39-54.
28. Martínez-Sabando, J., Coin, F., Melillo, J. H., Goyanes, S., & Cerveny, S. (2023). A review of pectin-based material for applications in water treatment. Materials, 16(6), 2207.
29. Banerjee, P., Sau, S., Das, P., & Mukhopadhayay, A. (2015). Optimization and modelling of synthetic azo dye wastewater treatment using Graphene oxide nanoplatelets: Characterization toxicity evaluation and optimization using Artificial Neural Network. *Ecotoxicology and environmental safety*, *119*, 47-57.
30. Fekete, T., Borsa, J., Takács, E., & Wojnárovits, L. (2017). Synthesis and characterization of superabsorbent hydrogels based on hydroxyethylcellulose and acrylic acid. *Carbohydrate polymers*, *166*, 300-308.
31. Gharekhani, H., Olad, A., Mirmohseni, A., & Bybordi, A. (2017). Superabsorbent hydrogel made of NaAlg-g-poly (AA-co-AAm) and rice husk ash: Synthesis, characterization, and swelling kinetic studies. *Carbohydrate polymers*, *168*, 1-13.
32. Peng, N., Wang, Y., Ye, Q., Liang, L., An, Y., Li, Q., & Chang, C. (2016). Biocompatible cellulose-based superabsorbent hydrogels with antimicrobial activity. *Carbohydrate polymers*, *137*, 59-64.
33. Khan, Y. H., Islam, A., Sarwar, A., Gull, N., Khan, S. M., Munawar, M. A., ... & Jamil, T. (2016). Novel green nano composites films fabricated by indigenously synthesized graphene oxide and chitosan. *Carbohydrate Polymers*, *146*, 131-138.
34. Paulchamy, B., Arthi, G., & Lignesh, B. D. (2015). A simple approach to stepwise synthesis of graphene oxide nanomaterial. J Nanomed Nanotechnol, 6(1), 1.
35. Khan, Y. H., Islam, A., Sarwar, A., Gull, N., Khan, S. M., Munawar, M. A., ... & Jamil, T. (2016). Novel green nano composites films fabricated by indigenously synthesized graphene oxide and chitosan. Carbohydrate Polymers, 146, 131-138.
36. Akalin, G. O., Oztuna Taner, O., & Taner, T. (2022). The preparation, characterization and antibacterial properties of chitosan/pectin silver nanoparticle films. Polymer

Bulletin, 79(6), 3495-3512.
37. Karimi Sani, I., Alizadeh, M., Pirsa, S., & Moghaddas Kia, E. (2019). Impact of operating parameters and wall material components on the characteristics of microencapsulated Melissa officinalis essential oil. *Flavour and Fragrance Journal*, *34*(2), 104-112.
38. Liu, X., Zhou, Y., Nie, W., Song, L., & Chen, P. (2015). Fabrication of hydrogel of hydroxypropyl cellulose (HPC) composited with graphene oxide and its application for methylene blue removal. *Journal of materials science*, *50*, 6113-6123.
39. Hassan, A., Niazi, M. B. K., Hussain, A., Farrukh, S., & Ahmad, T. (2018). Development of anti-bacterial PVA/starch based hydrogel membrane for wound dressing. *Journal of Polymers and the Environment*, *26*, 235-243.
40. Fematt-Flores, G. E., Aguiló-Aguayo, I., Marcos, B., Camargo-Olivas, B. A., Sánchez-Vega, R., Soto-Caballero, M. C., ... & Rodríguez-Roque, M. J. (2022). Milk protein-based edible films: Influence on mechanical, hydrodynamic, optical and antioxidant properties. Coatings, 12(2), 196.
41. Croitoru, A. M., Ficai, A., Ficai, D., Trusca, R., Dolete, G., Andronescu, E., & Turculet, S. C. (2020). Chitosan/graphene oxide nanocomposite membranes as adsorbents with applications in water purification. Materials, 13(7), 1687.
42. Gul, W., & Alrobei, H. (2021). Effect of graphene oxide nanoparticles on the physical and mechanical properties of medium density fiberboard. Polymers, 13(11), 1818.
43. Joel, J. M., Barminas, J. T., Riki, E. Y., Yelwa, J. M., & Edeh, F. (2018). Extraction and characterization of hydrocolloid pectin from goron tula (Azanza garckeana) fruit. World Sci. News, 101, 157-171.
44. Valencia, C., Valencia, C. H., Zuluaga, F., Valencia, M. E., Mina, J. H., & Grande-Tovar, C. D. (2018). Synthesis and application of scaffolds of chitosan- graphene oxide by the freeze-drying method for tissue regeneration. Molecules, 23(10), 2651.
45. Sivashankari, P. R., Krishna Kumar, K., Devendiran, M., & Prabaharan, M. (2021). Graphene oxide-reinforced pectin/chitosan polyelectrolyte complex scaffolds. Journal of Biomaterials Science, Polymer Edition, 32(17), 2246- 2266.
46. Kumar, S., & Koh, J. (2012). Physiochemical, optical and biological activity of chitosan-chromone derivative for biomedical applications. International journal of molecular sciences, 13(5), 6102-6116.
47. Sivashankari, P. R., Krishna Kumar, K., Devendiran, M., & Prabaharan, M. (2021). Graphene oxide-reinforced pectin/chitosan polyelectrolyte complex scaffolds. Journal of Biomaterials Science, Polymer Edition, 32(17), 2246- 2266.
48. Ain, Q. T., Haq, S. H., Alshammari, A., Al-Mutlaq, M. A., & Anjum, M. N. (2019). The systemic effect of PEG-nGO-induced oxidative stress in vivo in a rodent model. Beilstein journal of nanotechnology, 10(1), 901-911.
49. El Rouby, W. M., Farghali, A. A., Sadek, M. A., & Khalil, W. F. (2018). Fast removal of Sr (II) from water by graphene oxide and chitosan modified graphene oxide. Journal of Inorganic and Organometallic Polymers and Materials, 28, 2336-2349.